Effect of Water on the Electron Transfer Dynamics of 9-Anthracenecarboxylic Acid Bound to TiO_2 Nanoparticles: Demonstration of the Marcus Inverted Region

Ignacio Martini, José H. Hodak, and Gregory V. Hartland*

Department of Chemistry and Biochemistry, University of Notre Dame, Notre Dame, Indiana 46556

Received: September 8, 1997; In Final Form: November 15, 1997[⊗]

The electron transfer dynamics for 9-anthracenecarboxylic acid bound to nanometer-sized TiO_2 particles has been examined by transient absorption and time-resolved anisotropy measurements. The results from these experiments show that the forward electron transfer reaction occurs within the laser pulse, i.e., with a time constant of ≤350 fs. In absolute ethanol solutions the reverse electron transfer reaction occurs on a 33 ± 2 ps time scale. Addition of small amounts of water to the TiO_2/ethanol solutions produces a red shift in the absorbance spectrum of the TiO_2 particles and increases the overall rate of back electron transfer. This effect is attributed to the existence of oxygen vacancy defect sites at the surface of the TiO_2 particles. These defects produce Ti(III) centers which have an excess electron in a nonbonding t_{2g} orbital. When water is added to the sample, the Ti(III) surface atoms are converted to Ti(IV)−OH_2 groups. This removes the excess electrons and allows the low-energy t_{2g} orbitals to participate in the absorption of light, as well as in the back electron transfer reaction. The observation that the back electron transfer reaction is faster when these lower energy states are available proves that the back-reaction is an example of a Marcus inverted region reaction. A reorganization energy of 0.75 ± 0.05 eV was obtained for the back electron transfer reaction by using a two-state model, where the relative population of the lower energy state was determined by the amount of water added and the difference in energy between the states was taken from the UV/vis absorption spectrum. Both the forward and the reverse reactions have faster time constants than the corresponding reactions in our previous study of 9-anthracenecarboxylic acid bound to TiO_2. This difference arises because the TiO_2 samples in these two studies were prepared by different synthetic techniques. This leads to different structures for the TiO_2 surfaces and, therefore, different electronic coupling elements with the adsorbed dye molecules.

Introduction

The dye sensitization of wide bandgap semiconductor nanoparticles has received considerable attention in the past decade.[1−3] These systems are technologically important in photography and xerography via photoinduced electron transfer. In addition, the visible photoresponse of dye-sensitized semiconductor particles makes them good candidates for solar energy conversion and storage.[1−3] The use of nanoparticles in solar cells has the advantage over solid electrode surfaces in that nanoparticles provide the highest possible surface-to-volume ratio, therefore, maximizing the number of adsorbed dye molecules per unit volume of semiconductor.[2] Solutions of nanoparticles are also optically transparent, making it possible to study the fundamental electron transfer process by standard ultrafast laser techniques. Previous studies have shown that, upon excitation of the adsorbed dye, an electron is transferred to the conduction band of the semiconductor on a very fast time scale.[4−8] This is followed by trapping of the electron to sites at the surface of the particle.[9−11] For isolated semiconductor particles in solution the trapped electrons eventually undergo back electron transfer to the dye radical cation or reduce a different species at the particle surface.[12]

The forward electron transfer rate constant is controlled by the coupling of the excited state of the dye to the conduction band energy levels in the semiconductor. Because these energy levels are effectively continuous, the forward electron transfer reaction is expected to be extremely rapid.[3] Indeed, all ultrafast studies of the forward electron transfer reaction have determined time constants of ≤200 fs.[4−8] On the other hand, the back-reaction is thermally activated and is believed to lie in the Marcus inverted region, as proposed by Moser and Grätzel to explain their temperature-dependent studies of the back electron transfer reaction from TiO_2 particles to three different sensitizers.[13] Hupp and co-workers have more conclusively shown that the back electron transfer reaction is a Marcus inverted reaction by examining TiO_2 particles photosensitized by a series of ferricyanide complexes with different reduction potentials.[14] In general, a much wider range of time constants has been observed for the back electron transfer reaction compared to the forward electron transfer process; see, for example, refs 13−16. This has important consequences for solar energy conversion applications. The photoconversion efficiency is controlled by the ratio of k_f/k_b, where k_f and k_b are the rate constants for the forward and reverse electron transfer reactions, respectively. k_f is similar for most dye−semiconductor systems ($1/k_f$ on the order of 0.1−0.2 ps), while k_b varies by many orders of magnitude. For example, the time constant for back electron transfer in cresyl violet−SnO_2 is 12 ps,[15] whereas, the time constant for coumarin 343−TiO_2 is ca. 1 μs.[13] Thus, to maximize the photoconversion efficiencies of dye-sensitized semiconductor systems, it is clearly important to understand what factors control the time scale for the back electron transfer reaction.

In this paper we present a study on the electron transfer dynamics of 9-anthracenecarboxylic acid (9AC) bound to TiO_2

* Corresponding author. e-mail: hartland.1@nd.edu.

[⊗] Abstract published in *Advance ACS Abstracts,* December 15, 1997.

S1089-5647(97)02925-8 CCC: $15.00
Published on Web 01/15/1998

particles in absolute ethanol. We have determined that the time constant for the forward electron transfer reaction is less than 350 fs by comparing the time-resolved anisotropy of the bound dye to the anisotropy of the free dye in solution. This is in contrast to an earlier study of 9AC bound to TiO_2 particles that were prepared by a different technique, where we determined that the forward electron transfer time was ~1 ps.[16] This difference arises from a difference in the electronic coupling between the dye and the two TiO_2 samples. We also compare the rate of back electron transfer for different amounts of water added to the ethanolic solution. The results show a considerable increase in the rate of back electron transfer upon addition of small amounts of water (~1%). This is attributed to a change in the energy distribution of the trap sites at the semiconductor surface by the added water. The water also produces a red shift in the absorption spectrum of the TiO_2 particles, which shows that these trap sites are lower in energy. The increase in the rate constant for back electron transfer when lower energy trap sites are available proves that the reaction lies in the Marcus inverted region. Using a two-state model, we estimate a solvent reorganization energy of 0.75 ± 0.05 eV from the rate constants obtained in the ultrafast experiments and the observed shifts in the absorption spectra of the particles. These experiments show that the back electron transfer reaction is very sensitive to the chemical nature of the particle surface.

Experimental Section

The ultrafast transient absorption decays were measured with a regeneratively amplified mode-locked Ti:sapphire laser system (Clark-MXR CPA-1000; 100−120 fs fwhm $sech^2$ deconvolution; 0.6 mJ/pulse; $\lambda = 780$ nm). The laser system and experimental geometry have been described in detail in recent publications.[16,17] Briefly, the 780 nm output of the regenerative amplifier is split by a 90−10 beam splitter (CVI). The 90% portion is doubled in a 1 mm type I BBO crystal to supply the pump pulses (390 nm). The 10% portion is used as the probe beam, after being strongly filtered by neutral density filters. To control the polarization of the laser pulses, the pump and probe beams were passed through $\lambda/2$ achromatic waveplates (Special Optics) and Glan-Laser calcite polarizers (Karl-Lambrecht). The probe beam was split into signal and reference beams which were detected by matched large-area photodiodes (Thorlabs) for shot-to-shot normalization. The normalization, data collection, and analysis routines used for these experiments have been described elsewhere.[16,17]

The TiO_2 particle solutions were prepared following previously published synthetic methods.[9,18,19] One milliliter of titanium(IV) isopropoxide (ACROS, 98%) was dissolved into 20 mL of 2-propanol. This solution was slowly added (3 mL/min) to 200 mL of acidified water (with 1.2 mL of concentrated HNO_3) at 1 °C under N_2 (air was previously removed from the solution by boiling for 5 min). Mili-Q quality water (resistivity >18 MΩ) was used to avoid impurities in the final TiO_2 sample. After stirring for 3−4 h the solvent was removed by rotary evaporation at a temperature lower than 40 °C. The resulting white powder was dried under vacuum overnight. KOH was placed in the desiccator to help remove the excess HNO_3. The particle size was estimated to be 2 nm in diameter, based on comparison of the absorption spectrum to previously published spectra.[18,19] The crystalline structure of the semiconductor particles produced by this synthesis was examined by recording X-ray powder diffraction patterns in reflection mode with a Scintag X1 diffractometer, using a zero background quartz sample holder. Our samples show a broad peak at 25.3°, which is consistent with an anatase structure. However, the peak is extremely weak, which implies that the particles may be mostly amorphous. Synthesis yields, calculated as the mass of the dried white powder over the theoretical mass of TiO_2 produced in the synthesis, were approximately 200%. This indicates that the final sample contains many isopropoxide groups from the synthesis. Thermal gravimetric analysis (TA Instruments, SDT 2960) of the sample showed that half the sample weight evaporated at temperatures between 50 and 100 °C. This is consistent with TiO_2 particles that have a large number of loosely bound isopropoxide groups at their surface. The solutions used in the ultrafast and steady-state studies were obtained by redissolving the dried powder in absolute ethanol and adding 9-anthracenecarboxylic acid (Aldrich). Final concentrations of TiO_2 and 9AC were 0.35 g/L and 0.2 mM, respectively. Note that no attempt was made to remove oxygen from the sample after the initial synthesis. Steady-state absorption spectra were recorded using a Perkin-Elmer Lambda 6 UV/visible spectrophotometer.

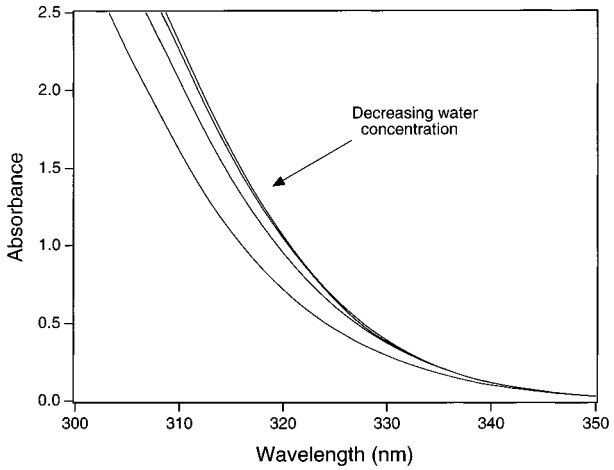

Figure 1. Absorption spectra of TiO_2 nanoparticles in ethanol with different water concentrations. From bottom to top the concentrations of water are 0%, 0.33%, 0.66%, and 1%.

Results

Steady-State Spectra. Figure 1 shows the absorption spectra of TiO_2 solutions (0.35 g/L) in absolute ethanol and with different concentrations of water. There is a clear red shift in the absorption spectra of TiO_2 upon addition of small quantities of water (0−1 vol %). This shift occurs instantaneously when the water is added and seems to be irreversible. No effect on the absorption spectrum of TiO_2 was found by changing the pH of the ethanolic solution from 2 to 5 by adding KOH. This agrees with the observations made by Bahnemann and coworkers of very little change in the TiO_2 absorption spectrum with pH for this specific TiO_2 synthesis procedure (hydrolysis of titanium(IV) isopropoxide in acidified water).[9]

The absorption spectra of the 9AC−TiO_2 solutions as a function of water concentration are shown in Figure 2a. The TiO_2 absorbance shows the same behavior as in Figure 1, as can be seen in the short wavelength part of the scans ($300 < \lambda < 320$ nm). For the 9AC molecules there is a small shift in the whole spectrum: the spectrum moves closer to the position of the free dye in solution as the concentration of water increases. Note that all these spectral shifts reach "saturation" at very small amounts of added water. Typically, preparing solutions with more than 2% water does not introduce further changes in either the absorption spectrum of TiO_2 or the ultrafast dynamics (vide infra). Figure 2b shows the absorption spectra of 9AC bound to the TiO_2 particles used in this study (sample

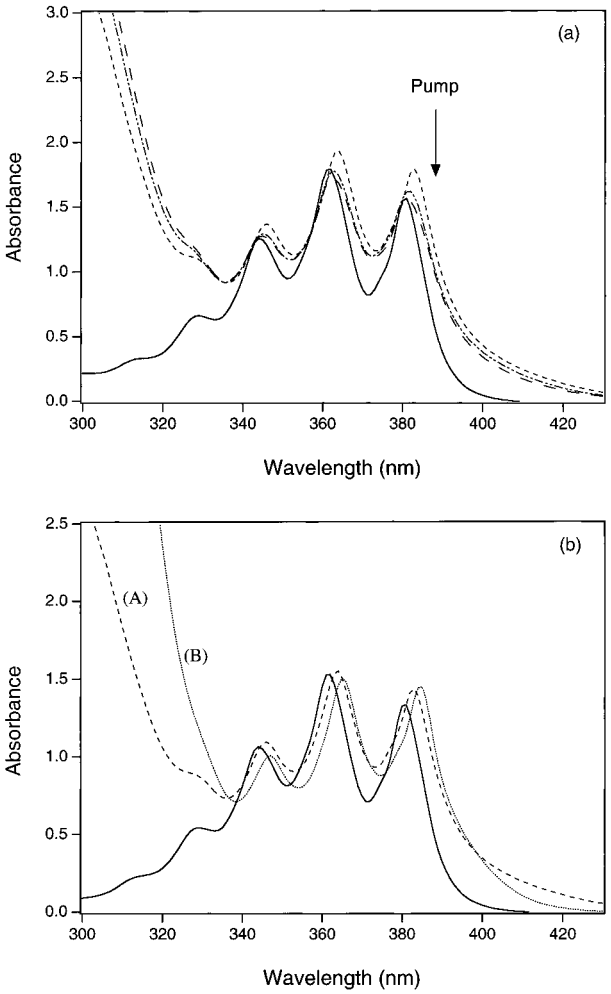

Figure 2. (a) Absorption spectra of 9AC (—) and 9AC adsorbed onto TiO_2 nanoparticles in ethanol with different concentrations of water: 0% water (---), 0.5% (— · · —), and 1% (— — —). (b) Absorption spectra of 9AC−TiO_2 for different TiO_2 samples: (A) particles used in the present study; (B) particles used in our previous work (see ref 16).

A) and the TiO_2 particles of our previous work (sample B), which were synthesized by rapidly adding titanium(IV) isopropoxide to ethanol. The concentration of TiO_2 is the same for both samples. Note that the onset of the TiO_2 absorption is different for the two samples and that the absorption spectrum of the bound dye is broader for the type A TiO_2 sample used in our present study. Specifically, the dye absorption extends much further into the visible spectral region (λ > 400 nm) for the type A particles. The difference in the absorption onset for the two TiO_2 samples is consistent with sample A having an anatase structure and sample B having a rutile structure.[9] However, powder X-ray diffraction patterns of the type B TiO_2 particles failed to show any peaks, which implies that the sample is amorphous.

Transient Absorption and Time-Resolved Anisotropy Measurements. Ultrafast transient absorption data for 9AC adsorbed onto the TiO_2 particles are shown in Figure 3, again as a function of water concentration. The pump laser wavelength for these experiments was 390 nm, and the probe laser wavelength was 780 nm. At this probe wavelength the electronically excited dye molecules, the dye radical cation, and the trapped conduction band electrons all contribute to the signal.[16] The decay in the transient absorption data is assigned to the back electron transfer reaction which destroys the $9AC^{\bullet+}$ radical cation and the trapped electrons. All the scans presented

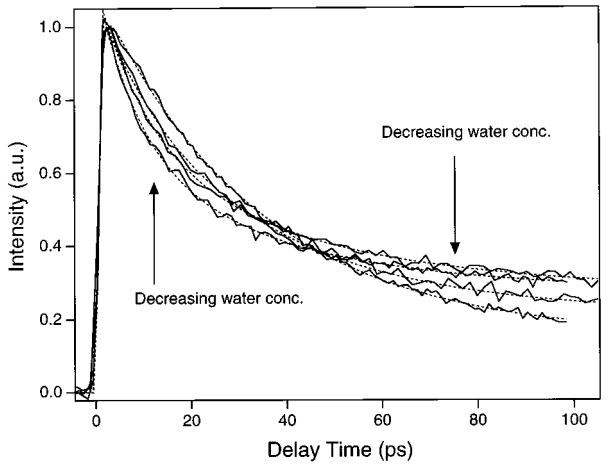

Figure 3. Transient absorption data for 9AC−TiO_2 recorded at the magic angle. The different concentrations of water are 0%, 0.2%, 0.5%, and 1%. The solid lines are the experimental data, and the dashed lines are the fits. The results of the fits are summarized in Table 1.

TABLE 1: Best Fit Values for the Data Presented in Figure 3

% water[a]	A_0	A_1	τ_1 (ps)[b]	A_2	τ_2 (ps)	$\bar{\tau}$ (ps)[c]	f[c]
0	0.14	0.86	32.9 ± 2			32.9	0
0.2	0.19	0.59	33f	0.21	8.2 ± 0.3	26.5	0.26
0.5	0.26	0.42	33f	0.33	7.7 ± 0.3	21.9	0.44
1	0.26	0.34	33f	0.39	8.7 ± 0.3	20.0	0.53
2	0.27	0.31	33f	0.42	8.7 ± 0.3	19.0	0.57
4	0.31	0.30	33f	0.39	8.9 ± 0.3	19.3	0.57

[a] The transient absorption data for the 2% and 4% water solutions are not shown in Figure 3 for space reasons. [b] The numbers in this table that are followed by an "f" are fixed parameters, they were not optimized by the fitting routine. [c] $\bar{\tau}$ and f are defined in the text.

in Figure 3 were measured at the magic angle (54.7°) to eliminate effects due to rotation.[20] Fits to the data using a function $S(t) = A_0 + A_1e^{-t/\tau_1} + A_2e^{-t/\tau_2}$ are also presented in Figure 3. This function consists of an offset (amplitude A_0) and one or two exponential decays (time constants τ_1, τ_2 and amplitudes A_1, A_2) and is convoluted with a 350 fs Gaussian pulse. The 350 fs instrument response function was determined from the instantaneous electronic response of pure ethanol in optical Kerr effect measurements. The results from the fits are summarized in Table 1. Note that adding water to the 9AC−TiO_2 solutions has two major effects on the dynamics. First, the average decay time $\bar{\tau} = (A_1\tau_1 + A_2\tau_2)/(A_1 + A_2)$ decreases monotonically from 33 to 19 ps as the percentage of water increases from 0% to 4%; see Table 1. Second, the relative amplitude of the offset (A_0) increases as the amount of added water increases.

The dynamics for 9AC−TiO_2 in pure ethanol, for the 1% water solution and for the free dye in solution, were also examined using parallel and perpendicular relative polarizations for the pump and probe laser pulses. The data from these experiments was used to calculate the time-resolved anisotropies, which are shown in Figure 4. Note that the anisotropy is negative for the bound dye molecules and positive for the free dye. The negative anisotropy signal is a signature of the $9AC^{\bullet+}$ radical cation.[16] Also shown in Figure 4 are single-exponential decays with time constants of 33 ps that roughly estimate the decay for the 9AC−TiO_2 time-resolved anisotropy signals. The anisotropy measurements confirm the assignment of the decay in the transient absorption data as due to the back electron transfer process, as we discussed in a recent publication[16] and is explained in the next section.

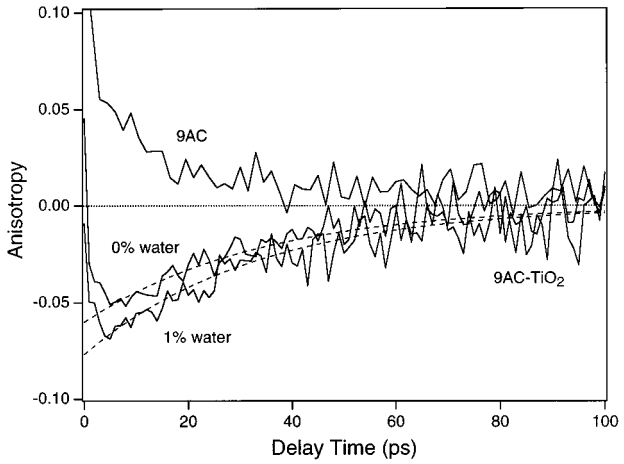

Figure 4. Time-resolved anisotropy decays for free 9AC and 9AC−TiO_2 in absolute ethanol and 1% water. Solid lines are the experimental data, and the dashed lines are 33 ps single-exponential decays that estimate the experimental decay.

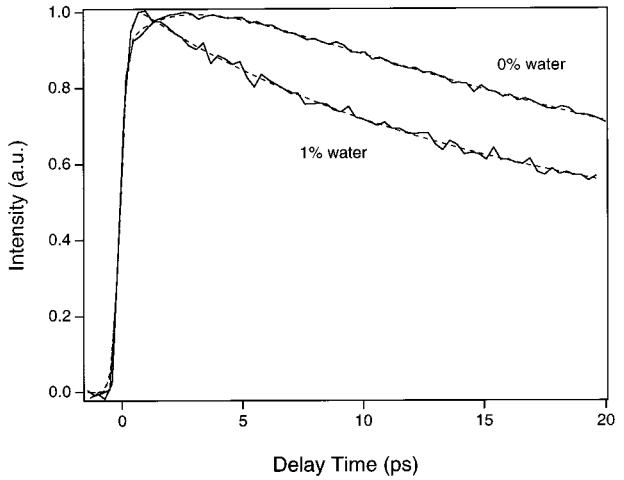

Figure 5. Short time dynamics for 9AC−TiO_2 in absolute ethanol and 1% water. Solid lines are the experimental data, and dashed lines are best fits for the data (see text for details).

Higher time resolution magic angle scans are presented in Figure 5 to show the difference in the short time dynamics for the 0% and 1% water solutions. These scans were fit using the parameters given in Table 1 with an additional exponential to account for the rise in the signal for the 0% water sample. The time constant for the exponential rise is 2.3 ps, and the rise accounts for 17% of the signal. It is important to note that the signal for the 1% water solution essentially rises with the laser pulse and then decays. Short time parallel and perpendicular pump−probe polarization scans and the corresponding anisotropies are shown in Figures 6 and 7, respectively, for the 0% and 1% water solutions. These scans show that the negative anisotropy signal is present within the instrument response time. Thus, the time scale for the forward electron transfer reaction must be ≤350 fs for this system. In addition, the anisotropy measurements show that the forward electron transfer rate constant is the same for the 0% and 1% water solutions (to within our time resolution).

Discussion

Steady-State Spectra. Different explanations were considered to justify the TiO_2 spectral shifts shown in Figures 1 and 2. We analyze first the ones we discarded: (i) One possibility is that addition of water causes particle growth. We believe

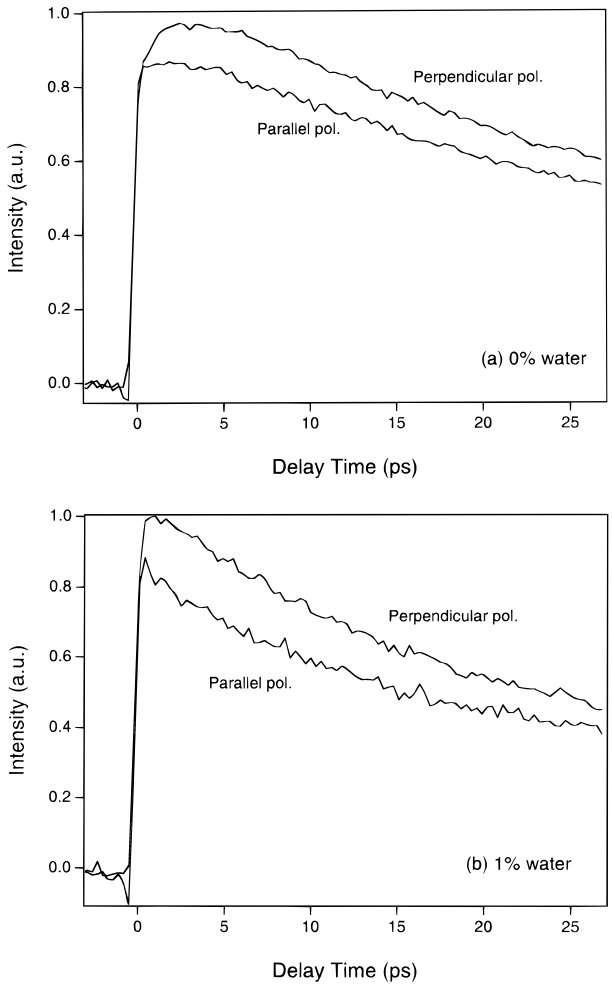

Figure 6. Short time transient absorption decays for 9AC−TiO_2 in (a) absolute ethanol and (b) 1% water solution, measured with parallel and perpendicular relative polarizations of the pump and probe laser pulses.

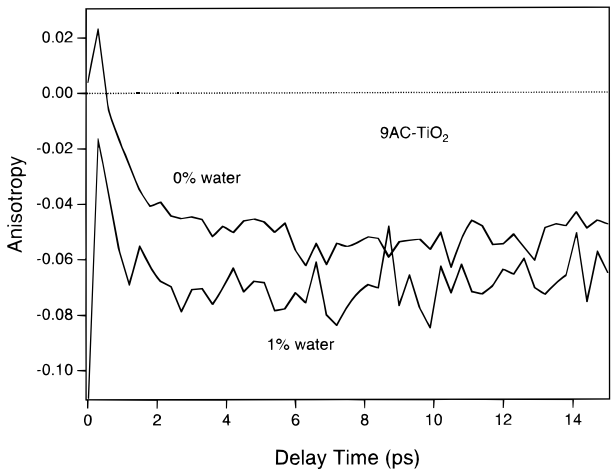

Figure 7. Time-resolved anisotropy data for 9AC−TiO_2 in absolute ethanol and 1% water solutions calculated from the transient absorption signals shown in Figure 6.

that growth in this system would occur by agglomeration rather than Ostwald rippening.[21] Particle agglomeration typically leads to precipitation; however, the solutions with water are stable for several weeks. Thus, although this mechanism of red-shifting the absorption spectrum cannot be completely discarded, we feel that it is unlikely to account for our observations. (ii) A second possibility is that water changes the surface charge,

which causes a change in the energy of the electron−hole exciton produced by photon absorption.[22] However, the magnitude of the observed red shift is much larger than the one expected from a pure electrostatic effect.[23] In addition, changing the charge on the surface of the particles by changing the pH of the ethanol solution with KOH showed almost no effect on the position of the absorption band, in agreement with previous studies.[9] Furthermore, the shift produced by using a basic water solution was almost identical with that produced by water alone. All these results indicate that it is the presence of water, and not the surface charge, that is the important factor in the bandgap shift. (iii) Another possibility is accumulation of conduction band electrons in the TiO_2 particles via bandgap excitation followed by hole scavenging. Isopropoxide groups, present from the synthesis (vide supra), could scavenge the valence band holes in the particles.[24] This mechanism would lead to an accumulation of conduction band electrons and, therefore, a blue shift in the absorption spectrum due to band filling. Replacement of the isopropoxide groups at the surface of the TiO_2 particles by water would decrease the steady-state concentration of conduction band electrons, because there would be fewer hole scavengers. However, the shift in the absorption spectrum occurs in the dark. In addition, the accumulation of conduction band electrons by this mechanism usually requires intense illumination and deoxygenated samples.[9] Therefore, band filling after bandgap illumination and hole scavenging was discarded as the mechanism for shifting the TiO_2 absorption onset.

Thus, we attribute the shift in the TiO_2 absorption spectrum to an interaction between the added water and surface defect sites. It is well documented in the literature that the most common defect found at titanium dioxide surfaces is an oxygen vacancy.[9,25−27] These vacancies result in Ti(III) centers at the surface that have an electron in a nonbonding t_{2g} orbital.[25−27] Calculations show that this excess electron is relatively localized around the oxygen vacancy and that the energy of the occupied Ti(III) t_{2g} orbitals is near the top of the bandgap, sometimes overlapping with the bottom of the conduction band.[25−27] These excess electrons are responsible for conductivity in heavily reduced TiO_2 surfaces.[26] The surface Ti(III) centers undergo a redox reaction with water to form Ti(IV)−OH_2;[9,25]

$$H_3O^+ + \text{Ti(III)} \rightarrow {}^1/_2H_2 + \text{Ti(IV)}-OH_2$$

i.e., the water molecules fill in the oxygen vacancy defect sites. Thus, the addition of water removes the excess electrons, which allows the previously occupied nonbonding Ti t_{2g} orbitals to participate in the absorption of light. This produces the red shift observed in the spectrum. It is not surprising that this effect is strong, considering that ∼30% of the TiO_2 molecules lie at the surface of the particles (assuming 2 nm diameter particles with a density equal to that for bulk TiO_2); i.e., the number of surface defects per particle can be very large. Another possibility is that the excess electrons are removed by O_2 to form O_2^-. This reaction occurs when water is added because O_2 has a greater solubility in water than in ethanol. However, experiments performed with deoxygenated water showed the same shift as with aerated water, which implies that O_2^- formation is not responsible for our observations.

Due to the strong interaction between the water molecules and semiconductor, some dye molecules are removed from the surface of the particles when water is added. (The water and the dye compete for surface Ti(III) atoms.) The basis for this statement is that the fluorescence intensity for the 9AC−TiO_2 samples increases with added water. The removal of bound dye molecules can also be seen in the 9AC absorption spectrum, which more closely resembles the spectrum of the free dye in solution when water is present. This is especially noticeable at the peaks of the absorption spectra, which are slightly red-shifted from the dye−semiconductor complex; see Figure 2a. However, the red tail of the 9AC absorption spectrum at ∼400 nm, which is due to adsorbed 9AC molecules that strongly interact with the TiO_2 surface, only shows a small decrease in intensity with added water. Therefore, only the weakly bound dye molecules (which do not have a large shift in their absorption spectra) are removed from the particle surface by the water molecules.

Time-Resolved Data. The 780 nm probe wavelength interrogates the $9AC^{\bullet+}$ radical cation, the excited electronic state of the dye, and the trapped electrons at the surface of the semiconductor nanoparticles.[11,16,28,29] For the pure ethanol solutions the free dye molecules in solution do not contribute significantly to the signal for the following reasons: (i) Due to the high association constant, over 90% of the 9AC molecules are bound to TiO_2.[16] (ii) The absorbance of the free dye molecules is ca. 5 times smaller than the absorbance of the bound dye molecules at the pump wavelength (Figure 2a). Consequently, at most 2% of the detected signal is due to free dye molecules. When water is added to the solution, the percentage of free dye molecules increases. These species have long-lived excited electronic states and are responsible for the increase in the relative amplitude of the offset; see Figure 3 and Table 1.

To explain the time-resolved data, we first focus on the short time scans. Figure 7 shows the transient anisotropy in the first 15 ps. The negative anisotropy signal has been assigned to the $9AC^{\bullet+}$ radical cation.[16] The measured anisotropy of the free dye in absolute ethanol is positive at zero time and decays biexponentially with time constants of ca. 1 and 10 ps, as shown in Figure 4.[16] The anisotropy in Figure 7 for the bound dye molecules becomes negative within the instrument response time (ca. 350 fs) for both the 0% and 1% water solutions; see also Figure 6. Thus, the forward electron transfer reaction occurs on a time scale of $\tau_f \leq 350$ fs. We recently reported a time constant for the forward electron transfer reaction of $\tau_f \sim 1$ ps for the same dye molecule adsorbed onto TiO_2 particles produced by a different synthesis procedure (hydrolysis of titanium(IV) isopropoxide in ethanol).[16] We attribute this difference in the forward electron transfer times to a difference in the electronic coupling of the dye to the semiconductor particles. This is corroborated by the UV/vis absorption spectra of 9AC bound to the two types of particles, which are shown in Figure 2b. Clearly the spectrum of 9AC bound to the type A particles used in the present study is much broader than that for the previous type B particles (see the $\lambda > 400$ nm spectral region). A broader spectrum implies a larger electronic coupling between the dye and the TiO_2 surface and, thus, a faster forward electron transfer reaction.[3] Note that we do not believe that the broadening is purely due to the shorter lifetime of the dye molecules bound to the type A particles; i.e., the spectra in Figure 2b have contributions from both homogeneous and inhomogeneous broadening.

The different electronic couplings may arise from a difference in the structure of the TiO_2 surfaces, which could affect the binding geometry for the adsorbed dye molecules. The powder X-ray diffraction patterns show that the present type A particles have greater crystallinity than the type B particles. The UV/vis absorption spectra of the TiO_2 samples (see Figure 2b) also show differences that can be attributed to different structures (type A corresponding to anatase and type B to rutile).[9] Thus,

it is reasonable to assume that the surface structure is different for the two types of particles.

Figure 5 shows that the 0% water TiO_2 sample has a 2.3 ps rise (which accounts for 17% of the signal) that is not observed in the 1% water sample. This rise is assigned to vibrational relaxation of the $9AC^{\bullet+}$ radical cation. The reason for this assignment is that the rise does not appear for the free dye. In addition, the time-resolved anisotropy measurements show that the radical cation is formed within 350 fs, which is much faster than the observed rise component. Thus, the rise must be due to dynamics of the radical cation, and the most likely possibility is vibrational relaxation. The rise is absent in the 1% water data probably due to a combination of three effects: (i) a faster back electron transfer reaction, (ii) a smaller contribution of $9AC^{\bullet+}$ to the signal, due to dissociation of some dye molecules from the surface, and (iii) possibly faster vibrational relaxation due to the presence of water at the TiO_2 surface. Note that because we are pumping at the red edge of the 9AC absorption spectrum, the photoexcited dye molecules initially have very little vibrational energy. Thus, the observation of a contribution from vibrational relaxation to the signal implies that the $9AC^{\bullet+}$ radical cation is produced with a significant amount of vibrational energy. This is not surprising as the ground state of the $9AC^{\bullet+}$ radical cation is much lower in energy than the S_1 state of the adsorbed dye. A time constant of 2.3 ps for vibrational relaxation at the surface of the TiO_2 particles is also consistent with our previous measurement of a 3 ps relaxation time for cresyl violet dimers at the surface of SnO_2 and SiO_2 particles.[15]

The long time scans shown in Figure 3 contain one- or two-exponential decays plus an offset which is due to adsorbed dye molecules that do not transfer an electron to the semiconductor particles or (for the samples with added water) to free dye molecules in solution. For the 0% water sample the 33 ± 2 ps single-exponential decay (τ_1 in Table 1) is consistent with the decay in the time-resolved anisotropy data presented in Figure 4. Therefore, this decay is assigned to the back electron transfer reaction.[16] Note that this time constant is smaller than the 54 ps time constant we reported for our previous study of 9AC−TiO_2. This difference again arises because the TiO_2 particles used in the two studies have different structures, which produces a difference in the electronic coupling elements for the adsorbed dye molecules and the radical cation. The faster back electron transfer time for the present study is consistent with the faster forward electron transfer time and the broadening observed in the 9AC−TiO_2 UV/vis absorption spectra. Strictly, the broadening in the absorption spectrum is related to the forward electron transfer reaction, not the back-reaction. However, it is reasonable to expect that the electronic coupling elements for the forward and reverse electron transfer reactions have a similar dependence on the properties of the TiO_2 surface.[3] Note that the back electron transfer time could also be affected by the particle diameter. Literature reports of the size of the particles produced by the two different synthesis techniques indicate that the type A particles are ca. 2 nm diameter and the type B particles are ca. 30 nm diameter.[9,11,30] Thus, for the type B particles the electrons will be initially trapped into sites that are, on average, further away from the dye radical cation. These electrons must diffuse across the surface before back electron transfer can occur. This will lead to a longer back electron transfer time for the larger particles.

The transient absorption signals for the samples prepared with small amounts of water were fitted to double-exponential decay functions. A double exponential was chosen over a single-exponential decay after performing an F test at the 1% significance level.[31] In these fits, τ_1 was held fixed to the value measured for pure ethanol and τ_2 was allowed to vary. τ_2 was found to be much smaller and can be considered constant at $\tau_2 = 8.3 \pm 0.7$ ps for the different scans, to within our signal-to-noise; see Table 1. The relative amplitude of the second exponential increases as the amount of added water increases; this decreases the average decay time $\bar{\tau}$ given in Table 1. Due to the poor signal-to-noise ratio for the anisotropy measurements, it is difficult to determine the presence of the second exponential in the 1% water data presented in Figure 4. However, it should be noted that the free dye presents a similar 10 ps decay that could cancel with τ_2 in the anisotropy measurements. We assign the 8.3 ps time constant to back electron transfer from trap sites at the particle surface that become available when water is added to the sample. In the next section we will demonstrate that these trap sites are the same as the ones that produce the red shift in the absorption spectrum; i.e., they are lower in energy than the sites that give rise to the 33 ps back electron transfer time.

Kinetic Model for Back Electron Transfer. To explain the double-exponential decay in the transient absorption signal, we propose a two-state model for sites at the TiO_2 surface. The sites that are initially present when only alkoxy groups are bound to the surface are designated as 1, and the surface sites produced by adding water are designated as 2. Our model for electron transfer at the surface of TiO_2 can be represented by the following scheme:

$$9AC \xrightarrow{h\nu} 9AC^* \tag{1}$$

$$9AC^* \xrightarrow{k_f} 9AC^{\bullet+} + e_{cb} \tag{2}$$

$$e_{cb} \xrightarrow{(1-f)k_t} e_{t_1} \tag{3a}$$

$$\xrightarrow{fk_t} e_{t_2} \tag{3b}$$

$$9AC^{\bullet+} + e_{t_1} \xrightarrow{k_1} 9AC \tag{4a}$$

$$9AC^{\bullet+} + e_{t_2} \xrightarrow{k_2} 9AC \tag{4b}$$

where 9AC* is the vibronically excited dye molecule produced by the pump laser, $9AC^{\bullet+}$ is the dye radical cation, e_{cb} is an electron in the conduction band of the semiconductor, e_{t_1} and e_{t_2} are electrons trapped at the two different sites, f is the fraction of e_{cb} that go to trap site 2, and k_f, k_t, k_1, and k_2 are the rate constants for forward electron transfer, trapping, and back electron transfer from the two different sites, respectively. Note that water converts the type 1 sites into type 2 sites. The signal detected, $S(t)$, arises from the dye radical cation, the excited state of the dye, and the trapped electrons.[11,16,28,29] Assuming that the electrons in the two trap sites have the same absorption coefficient at 780 nm, $S(t)$ is given by

$$S(t) = \alpha_1[9AC^*] + \alpha_2[9AC^{\bullet+}] + \alpha_3([e_{t_1}] + [e_{t_2}]) \tag{5}$$

where α_1, α_2, and α_3 are absorption coefficients for the electronically excited dye molecules, the dye radical cation, and the trapped electrons, respectively. The time-resolved anisotropy measurements presented in Figure 7 show that $1/k_f \leq 350$ fs. In addition, transient absorption measurements performed by directly exciting electron−hole pairs in TiO_2 particles yield

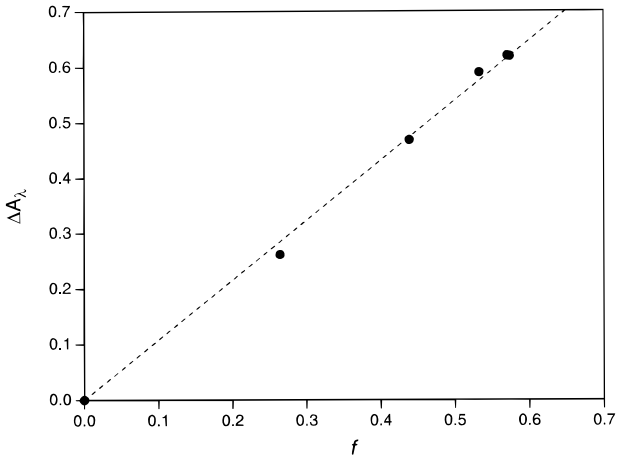

Figure 8. ΔA_λ versus f for different water/ethanol solutions. The maximum value of f corresponds to a 4% water solution; see text for details.

a value for the trapping time of $1/k_t \approx 100-200$ fs.[11,19] In contrast, the data presented in Figure 3 show that $1/k_1$ and $1/k_2$ are 33 and 8.3 ps, respectively. Thus, k_f, $k_t \gg k_1$, k_2. Given that the back electron transfer reaction is first order in e_t only, eqs 1−4 can be solved to give

$$S(t) = \alpha_1 C_0' + (1 - f)(\alpha_2 + \alpha_3)C_0 \exp(-k_1 t) + f(\alpha_2 + \alpha_3)C_0 \exp(-k_2 t) \quad (6)$$

where C_0 is the concentration of photoexcited dye molecules that undergo electron transfer, and C_0' is the concentration of dye molecules that remain electronically excited. (These species have nanosecond lifetimes and produce the offset in the transient absorption signal.) This equation reproduces the experimental observation of an offset plus a double-exponential decay. The ratio of C_0'/C_0 is determined by the amount of free dye in solution, as well as site heterogeneity at the TiO_2 surface. (We have previously shown that not all the adsorbed dye molecules undergo electron transfer; see ref 16.) Equation 6 shows that the ratio of the preexponential factors (A_2/A_1 in Table 1) is determined by f, the fraction of the type 2 sites (the sites created by adding water to the sample). Specifically, $A_2/A_1 = f/(1 - f)$. The values of f derived from the data are included in Table 1.

In addition to changing the back electron transfer rate, adding water to the sample causes a shift in the TiO_2 absorption spectrum. To verify that the sites that give rise to the red shift in the absorption spectrum are also responsible for the faster time scale decay, the absorbance of the TiO_2 particles is written as

$$A_\lambda = \epsilon_0 l[TiO_2] + \epsilon_1 l(1 - f)[TiO_2] + \epsilon_2 lf[TiO_2] \quad (7)$$

where ϵ_0 is the absorbance of the interior TiO_2 moieties, ϵ_1 and ϵ_2 are the absorption coefficients of the two surface sites, and l is the length of the sample cell. From eq 7, the change in absorbance for TiO_2 upon addition of water can be written as

$$\Delta A_\lambda = \Delta\epsilon l[TiO_2]f \quad (8)$$

where ΔA_λ is the difference in absorbance at wavelength λ and $\Delta\epsilon = \epsilon_2(\lambda) - \epsilon_1(\lambda)$.

Figure 8 shows a plot of ΔA_λ versus f, where ΔA_λ is determined from the UV/vis spectra, see Figure 2a, and f is calculated from the ratio of the exponential decays in the corresponding transient absorption traces (Table 1). λ was chosen to be 312 nm, i.e., a wavelength where the 9AC spectrum changes very little upon addition of water. The correlation factor for a linear fit is 0.999, which proves that there is a strong correlation between the changes in the steady-state spectra and the dynamics measurements. Note that a positive ΔA_λ corresponds to a red shift in the spectrum and that the effect of adding water saturates at $f = 0.57$; i.e., after ~2% water has been added to the TiO_2 solutions, there is no further change in either the steady-state spectra or the transient absorption traces.

This analysis explicitly shows that there is a 1:1 correspondence between the sites with a red-shifted absorption spectrum and the sites that have the faster back electron transfer time τ_2. The red shift in the TiO_2 absorption spectra was explained by a mechanism where water removes oxygen defect sites at the surface of the TiO_2 particles by forming Ti(IV)−OH_2 species. This process removes electrons from nonbonding Ti t_{2g} orbitals, which allows these orbitals to participate in the absorption of light and, so, produce the spectral red shift. Obviously, once the excess electrons have been removed, these Ti t_{2g} orbitals can also take part in the back electron transfer reaction. Note that the two-state model described above is a simplification of the actual energy distribution of sites at the TiO_2 surface. However, this is the simplest model that can give a biexponential decay for the back electron transfer reaction. In addition, for this model to be correct the excess electrons at the Ti(III) defect sites must be localized and unable to react with the dye radical cation. In contrast, electrons in levels associated with the Ti(IV)−OH_2 groups are reactive.

Reorganization Energy for Interfacial Electron Transfer. The conclusion from the two-state model is that the sites with an 8.3 ps back electron transfer time are lower in energy (they have a red-shifted absorption spectrum) compared to the sites with the 33 ps back electron transfer time. The fact that the back electron transfer reaction is faster from lower energy surface sites unambiguously shows that this reaction is in the Marcus inverted region. A simple formula for the electron transfer rate constant is[32]

$$k_b^i = \left(\frac{2\pi}{h}\right)|V|^2\sqrt{2\pi\Lambda k_b T}\exp\left(-\frac{(\Delta_r G_i^0 + \Lambda)^2}{4\Lambda k_b T}\right) \quad (9)$$

where V is the electronic coupling matrix element, $\Delta_r G_i^0$ is the free energy of the reaction for site i ($i = 1, 2$), and Λ is the reorganization energy. Assuming that V is the same for both trap sites, we can estimate the reorganization energy by taking the ratio of the back electron transfer rate constants for the two sites and calculating approximate values for $\Delta_r G_i^0$. For the higher energy site $\Delta_r G_1^0$ was calculated from the flatband potential of TiO_2, $E_{cb} = -0.5$ eV versus NHE at pH = 4 (ref 2), and the standard reduction potential of 9AC, $E(9AC/9AC^{\bullet+}) = 1.3$ eV versus NHE.[12,29] This yields $\Delta_r G_1^0 = -1.8$ eV. For the lower energy site $\Delta_r G_2^0$ was obtained by subtracting the difference in energy between sites 1 and 2 from $\Delta_r G_1^0$. This energy difference was estimated to be ~50 meV from the red shift in the onset of the UV/vis absorption spectra of the TiO_2 particles with added water, i.e., $\Delta_r G_2^0 = -1.75$ eV. With these values of $\Delta_r G_1^0$ and $\Delta_r G_2^0$ we calculate a reorganization energy of 0.75 ± 0.05 eV. Note that we have assumed that the red shift in the TiO_2 absorption spectrum is entirely due to changes in the conduction band energy levels. This assumption is consistent with our picture of the surface of TiO_2: the red shift in the spectrum and the increase in the back electron transfer rate occur because excess electrons are removed from nonbonding Ti(III) t_{2g} orbitals. Also, the value of 0.75 eV for the

reorganization energy is consistent with a previous measurement for interfacial electron transfer at the surface of a gold electrode.[33]

This demonstration of Marcus inverted behavior for electron transfer from TiO_2 to an adsorbed molecule is complementary to the study of Hupp and co-workers.[14] In Hupp's experiments the back electron transfer rate was measured as a function of the reduction potential of a series of ferricyanide molecules adsorbed onto TiO_2 particles, under conditions where there should be no change in the energetics of the TiO_2 surface sites. In our study the energy of the trapped electrons in the semiconductor particles was varied by modifying the particle surface, while keeping the adsorbate constant. Furthermore, Hupp and co-workers examined a system where the adsorbed molecules form a charge transfer complex with the TiO_2 particles; i.e., a new band is formed in the UV/vis spectrum when the ferricyanide molecules are attached to the particles. In contrast, adsorption onto TiO_2 modifies the 9AC UV/vis spectrum (it becomes broader and shifts to the red) but does not result in the formation of a new band. This is the more usual case in dye sensitization experiments with semiconductor particles. Also note that our measurements of rate constant versus relative energy are a direct confirmation of Marcus inverted behavior, as opposed to the indirect temperature-dependent studies of Moser and Grätzel.[13]

Note that we cannot completely rule out particle agglomeration as a contributing reason for the red shift in the TiO_2 absorption spectrum. However, even if this mechanism predominates, the conclusion that the back electron transfer reaction is in the Marcus inverted region does not change. This is because larger particles should show slower back electron transfer times, because the trapped electrons and the dye radical cation are separated by larger distances. This is contrary to our observations, which shows that energetics is the important factor in controlling k_b; i.e., the faster back electron transfer times with added water is due to a lower conduction band energy and Marcus inverted behavior. However, as stated above, we do not feel that aggregation is significant in our samples, due to their long-term stability.

Summary and Conclusions

The dynamics of electron transfer between 9AC and TiO_2 nanoparticles has been examined with ultrafast time resolution. The time constant for the forward electron transfer reaction was determined to be $\leq$350 fs, limited by the time resolution of the measuring system. This time constant is faster than the $\sim$1 ps forward electron transfer time obtained in our previous measurements, which used TiO_2 particles prepared by a different synthetic technique. This difference is due to a difference in the electronic coupling matrix element between 9AC and the two types of TiO_2 particles. In pure ethanol, the back electron transfer time was found to be 33 ± 2 ps, again faster than that in our previous study (54 ps). A small 2.3 ps rise was also observed in the transient absorption signal, which was assigned to vibrational relaxation of the $9AC^{\bullet+}$ radical cation; i.e., the electron transfer reaction creates vibrationally hot products.

When water is added to the samples, the decay of the radical cation signal becomes biexponential with time constants of 33 and 8.3 ± 0.7 ps. The relative amplitude of the 8.3 ps component increases as the amount of water in the TiO_2/ethanol solution increases. Adding water also produces a red shift in the TiO_2 absorption spectrum. There is a direct correlation between the red shift in the absorption spectrum and the relative amplitude of the 8.3 ps exponential in the transient absorption data. These observations can be explained by a two-state model where the site that gives the 8.3 ps decay time is lower in energy than the site that gives the 33 ps decay. Thus, our measurements provide a direct demonstration that the back electron transfer reaction for 9AC bound to TiO_2 is in the Marcus inverted region. Using the red shift in the UV/vis spectra to indicate the difference in energy between the two sites yields a reorganization energy of 0.75 ± 0.05 eV. In general, these experiments show that the rate of interfacial electron transfer can be very sensitive to small changes in the preparation of the semiconductor samples and the state of the surface.

Acknowledgment is made to the donors of the Petroleum Research Fund, administered by the American Chemical Society. I.M. would like to thank J. J. Johnson and D. Miller for their kind donation of glassware. We are also grateful to Prof. Paul McGinn for recording the X-ray powder patterns and thermal gravimetric analysis data for our samples. The X-ray and TGA facilities are supported by the NSF (CTS96-01780).

References and Notes

(1) Kamat, P. V. *Chem. Rev. (Washington, D.C.)* **1993**, *93*, 267.
(2) Hagfeldt, A.; Grätzel, M. *Chem. Rev. (Washington, D.C.)* **1995**, *95*, 49.
(3) Miller, R. J. D., McLendon, G. L., Nozik, A. J., Schmickler, W., Willig, F., Eds. *Surface Electron Transfer Processes*; VCH: New York, 1995.
(4) Rehm, J. M.; McLendon, G. L.; Nagasawa, Y.; Yoshihara, K.; Moser, J.; Grätzel, M. *J. Phys. Chem.* **1996**, *100*, 9577.
(5) Burfeindt, B.; Hannappel, T.; Storck, W.; Willig, F. *J. Phys. Chem.* **1996**, *100*, 16463.
(6) Tachibana, Y.; Moser, J. E.; Grätzel, M.; Klug, D. R.; Durrant, J. R. *J. Phys. Chem.* **1996**, *100*, 20056.
(7) Murakoshi, K.; Yanagida, S.; Capel, M.; Castner, E. W. ACS Symposium, Nanostructured Materials: Clusters, Composites and Thin Films, April 13−17, 1997.
(8) Cherepy, N. J.; Smestad, G. P.; Grätzel, M.; Zhang, J. Z. *J. Phys. Chem. B* **1997**, *101*, 9342.
(9) Bahnemann, D. W. *Isr. J. Chem.* **1993**, *33*, 115.
(10) Lanzafame, J. M.; Palese, S.; Wang, D.; Miller, R. J. D. *J. Phys. Chem.* **1994**, *98*, 11020.
(11) Skinner, D. E.; Colombo, D. P.; Cavaleri, J. J.; Bowman, R. M. *J. Phys. Chem.* **1995**, *99*, 7857.
(12) See, for example: Kamat, P. V. *J. Phys. Chem.* **1989**, *93*, 859.
(13) Moser, J. E.; Grätzel, M. *Chem. Phys.* **1993**, *176*, 493.
(14) Lu, H.; Prieskorn, J. N.; Hupp, J. J. *J. Am. Chem. Soc.* **1993**, *115*, 4927.
(15) Martini, I.; Hartland, G. V.; Kamat, P. V. *J. Phys. Chem. B* **1997**, *101*, 4826.
(16) Martini, I.; Hodak, J. H.; Hartland, G. V.; Kamat, P. V. *J. Chem. Phys.* **1997**, *107*, 8064.
(17) (a) Martini, I.; Hartland, G. V. *Chem. Phys. Lett.* **1996**, *258*, 180. (b) Martini, I.; Hartland, G. V. *J. Phys. Chem.* **1996**, *100*, 19764.
(18) Bahnemann, D.; Hanglein, A.; Lillie, J.; Spanhel, L. *J. Phys. Chem.* **1984**, *88*, 709.
(19) Colombo, D. P.; Roussel, K. A.; Saeh, J.; Skinner, D.; Cavaleri, J. J.; Bowman, R. *Chem. Phys. Lett.* **1995**, *232*, 207.
(20) Fleming, G. R. *Chemical Applications of Ultrafast Spectroscopy*; Oxford University Press: Oxford, 1986.
(21) Everett, D. H. *Basic Principles of Colloid Science*; Royal Society of Chemistry: London, 1988.
(22) Brus, L. E. *IEEE J. Quantum Electron.* **1986**, *QE-22*, 1909.
(23) Henglein, A.; Kumar, A.; Janata, E.; Weller, H. *Chem. Phys. Lett.* **1986**, *132*, 133.
(24) Dounghong, D.; Ramsden, J.; Grätzel, M. *J. Am. Chem. Soc.* **1982**, *104*, 2977.
(25) Henrich, V. E.; Cox, P. A. *The Surface Science of Metal Oxides*; Cambridge University Press: Cambridge, 1994.
(26) Ramamoorthy, M.; King-Smith, R. D.; Vanderbilt, D. *Phys. Rev. B* **1994**, *49*, 7709.
(27) Noguera, C. *Physics and Chemistry at Oxide Surfaces*; Cambridge University Press: Cambridge, 1996.
(28) Rothenberger, G.; Moser, J.; Gratzel, M.; Serpone, N.; Sharma, N. K. *J. Am. Chem. Soc.* **1985**, *107*, 8054.
(29) Kamat, P. V. *Langmuir* **1990**, *6*, 512.
(30) Kamat, P. V.; Chauvert, J.-P.; Fessenden, R. W. *J. Phys. Chem.* **1986**, *90*, 1389.
(31) Gans, P. *Data Fitting in the Chemical Sciences*; John Willey & Sons: West Sussex, 1992.
(32) Marcus, R. A.; Sutin, N. *Biochim. Biophys. Acta* **1985**, *811*, 265.
(33) Chidsey, C. E. D. *Science* **1991**, *251*, 919.